Polymer, 1991, Vol. 32, 146–159

Redox-active polymers by group-transfer polymerization: physical, electrochemical and electronic properties

André Laschewsky* and Michael D. Ward†
Central Research and Development Department, Experimental Station 328, E.I. du Pont de Nemours & Co., PO Box 80328, Wilmington, DE 19880-0328, USA
(Received 23 October 1989; accepted 2 December 1989)

A variety of redox-active polymers and copolymers containing *N,N,N',N'*-tetraalkyl-1,4-phenylenediamine were synthesized, preferentially based on methacrylates and sorbates. Group-transfer polymerization proved to be the polymerization method of choice, in order to protect the rather sensitive functional groups. Electrochemical studies indicated that oxidation of the redox-active group generally occurred at low oxidation potentials (~0.25 V vs. SCE), generating stable poly(radical ions). Structural variation of the polymers did not alter the redox behaviour significantly. Owing to their low oxidation potential, the polymers are easily oxidized, or form charge-transfer complexes with many electron acceptors. Whereas the native polymers are insulators, exhibiting electrical conductivities smaller than $10^{-12}\,\Omega^{-1}\,cm^{-1}$, exposure to iodine yielded materials that absorbed up to 85% iodine (w/w) with conductivities in the range 10^{-2} to $10^{-4}\,\Omega^{-1}\,cm^{-1}$. The conductivities measured are virtually equal for all polymers studied, being rather insensitive to the detailed polymer structure.

(Keywords: redox polymers; group transfer polymerization; Wurster's blue; TMPD; conductivity; cyclic voltammetry)

INTRODUCTION

Redox-active polymers[1,2] have been investigated in the past for various purposes, such as polymeric reagents or electronic materials. Two general classes of polymers can be distinguished, either characterized by conjugated polymer backbones, such as polyacetylene or polyaniline, or characterized by separated redox-active moieties, such as quinones, viologen or ferrocene. The latter class represents in general soluble polymers with well defined chemical structures, and thus enables detailed studies of the redox behaviour. *N,N,N',N'*-Tetramethyl-1,4-phenylenediamine (TMPD) has been studied thoroughly as a redox-active compound and is known to form a stable radical ion (Wurster's blue) upon oxidation[3–5]. Although the use of TMPD sites in a polymer framework appears promising since the oxidation potential of TMPD is low (+0.13 V vs. SCE in acetonitrile[5]), suggesting facile chemical and electrochemical doping and environmental stability of the resulting poly(radical ions), little work has been done on polymeric TMPD derivatives. Accordingly, TMPD derivatives bound to polymers via substitution at the nitrogen atoms were investigated with particular emphasis on the role of position and density of the TMPD groups in determining redox behaviour and electrical properties. The following structures represent possible formats for TMPD-containing polymers wherein structural properties can be systematically varied:

Scheme 1

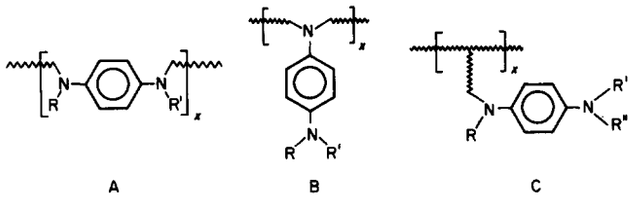

Some polymers of types A and B have been prepared by Klöpffer[6] and by Hörhold[7,8] via polyaddition reactions, but detailed studies of the redox properties are missing as yet. We have focused our main interest on type C polymers of various structure, including some type B polymers for comparative studies.

EXPERIMENTAL

General working conditions

Because all starting compounds and intermediates based on *p*-phenylenediamine are extremely sensitive to oxygen, all synthesis procedures were performed under nitrogen, and all solvents were degassed with nitrogen prior to use.

Materials

Tetrahydrofuran (THF) was distilled over sodium. All other solvents were dried by passing through neutral Al_2O_3 columns, and were stored in either a dry box or over molecular sieves. Column filtration was performed with either neutral Al_2O_3 ICN Alumina N–Akt.I (ICN Biomedicals) or basic Al_2O_3 ICN Alumina B–Akt.I, silica

* Present address: Institute of Organic Chemistry, University of Mainz, D-6500, Mainz, FRG
† To whom correspondence should be addressed at current address: Department of Chemical Engineering and Material Science, University of Minnesota, Admondson Hall, 421 Washington Avenue S.E., Minneapolis, MN 55455, USA

0032-3861/91/010146-14

gel Kieselgel 60 (230–400 mesh, EM Science). Melting points are uncorrected.

Synthesis of starting materials

4-Dimethylaminoaniline, DMPD (**1**). DMPD was purchased from Aldrich and Fluka. The black waxy solid was purified by distillation under reduced pressure, b.p. (0.1–0.5 mmHg) ~ 60–80°C. It was a colourless, waxy solid; m.p. = 53°C.

N-(*4-Dimethylaminophenyl*)*formamide, DMPD-Fa* (**2**). 235 g of distilled DMPD were refluxed with 900 ml benzene and 86.1 g formic acid in a Dean–Stark water trap for 3 days. On cooling at 5°C, a yellow precipitate was formed. The raw product was recrystallized from toluene, to give colourless needles. Yield, 232 g (82%); m.p. = 108°C.

N,N,N′-*Trimethyl-1,4-phenylenediamine, TriMPD* (**3**). 39 g $LiAlH_4$ were suspended in 700 ml dry THF at room temperature. 200 g *N*-(4-dietmylaminophenyl)formamide suspended in 800 ml THF were added over 2–3 h, so that the mixture boils gently only. The mixture was stirred for 1 h at room temperature, and for 1 h at reflux. After cooling by an ice bath, 7.5 ml ethyl acetate followed by 74 ml ice water were added slowly, while stirring and cooling. After standing overnight, the mixture was filtered to yield a filtrate (which was saved) and a precipitate, which was isolated and heated at reflux in 500 ml THF for 12 h. This mixture was then filtered and filtrates were combined. Evaporation of the solvent gave a brownish oil, which was fractionally distilled over a 20 cm Vigreux column to yield 129 g (70%) of colourless oil; b.p. (0.1 mmHg) ~ 80–88°C; $n_D^{22} = 1.5829$. High-resolution mass spectrum: signal at mass 150.1150; calculated for $C_9H_{14}N_2$, 150.1157. ^{1}H n.m.r. (solvent $CDCl_3$), δ (ppm): 2.8 broadened s (9H, $(CH_3)_2$–N–, CH_3–N–); 3.18 broad s (0.8H, –NH?); 6.55–6.8 m (4H, N–C_6H_4–N). Product stains deep purple in air.

N,N,N′,N′-*tetramethyl-1,4-phenylenediamine, TMPD* (**4**). TMPD was purchased as the dihydrochloride salt (Aldrich). The free base was obtained by dissolving the dihydrochloride in oxygen-free water, placing diethyl ether above the aqueous phase, and adding NaOH (5% surplus). The colourless precipitate was extracted, the organic phase separated, dried over Na_2SO_4, and the solvent evaporated, yielding a colourless powder; m.p. = 50°C. Product stains deep blue in air.

trans-*4,4′-Bis*(*dimethylamino*)*stilbene, TMSt* (**5**). TMSt was prepared according to Stewart[9]. Recrystallization from 4/1 (v/v) toluene/chloroform and from toluene gave yellow needles; m.p. = 268–369°C. Solutions of TMSt are strongly fluorescent. High-resolution mass spectrum: signal at mass 266.1775; calculated for $C_{18}H_{22}N_2$, 266.1783. ^{1}H n.m.r. (solvent DMSO-d_6), δ (ppm): 2.9 s (12H, $(CH_3)_2$N–); 6.7 d (2H, –C_6H_4–N); 6.85 s (2H, –CH=CH–); 7.28 d (2H, –C_6H_4–C).

Bis-4,4′-(*dimethylamino*)*azobenzene, TMAzo* (**6**). TMAzo was prepared according to Nölting[10]. Repeated recrystallization from toluene gave orange needles; m.p. = 282–283°C. High-resolution mass spectrum: signal at mass 268.1681; calculated for $C_{16}H_{20}N_4$, 268.1688. ^{1}H n.m.r. (solvent $CDCl_3$), δ (ppm): 3.05 s (12H, $(CH_3)_2$N–); 6.75 d (2H, –C_6H_4–N); 7.82 d (2H, –C_6H_4–N=N).

N-(*4′-Dimethylaminophenyl*-N-*methyl-2-aminoethanol, T2OH* (**7**). In the stainless-steel pressure vessel three batches of 37.6 g TriMPD (**3**) and 12 g ethylene oxide, 59 g/19 g and 64.2 g/20 g were reacted for 36 h at 80°C. The liquid reaction products were combined, and fractionated by distillation to yield 174.3 g (84%) slightly yellow oil; b.p. (0.2 mmHg) = 125–140°C; $n_D^{25} = 1.5789$. High-resolution mass spectrum (trimethylsilyl derivative): signal at mass 266.1815; calculated for $C_{14}H_{26}N_2OSi$, 266.1814. ^{1}H n.m.r. (solvent $CDCl_3$), δ (ppm): 2.84 s (3H, CH_3–N); 2.88 s (6H, $(CH_3)_2$N–); 3.28 t (2H, –CH_2–N–); 3.75 t (2H, –CH_2–O–); 6.75–6.9 m (4H, –C_6H_4–).

N-(*4′-Dimethylaminophenyl*)-N-*methyl-3-aminopropanol, T3OH* (**8**). 75.8 g TriMPD (**3**), 75.8 g ethyl acrylate and 1 ml acetic acid were heated for 16 h. The mixture was cooled, and 400 ml THF added. A suspension of 18 g $LiAlH_4$ in 200 ml THF was added slowly so that the mixture boiled gently. The mixture was stirred for 1 h at room temperature, heated to reflux for 1 h and cooled to 0°C. Then 32 g ethyl acetate were added cautiously, followed by 38 g ice water. After standing overnight the precipitate was filtered and heated to reflux in 400 ml THF for 4 h, and the mixture filtered again. The filtrates were combined and evaporated. The residual oil fractionally distilled in vacuum yields 66.8 g (64%) of a slightly yellow oil: b.p. (0.1 mmHg) = 134–138°C. High-resolution mass spectrum (trimethylsilyl derivative): signal at mass 280.2009; calculated for $C_{15}H_{28}N_2OSi$, 280.1971. ^{1}H n.m.r. (solvent $CDCl_3$), δ (ppm): 1.85 m (2H, –CH_2–); 2.85 s (3H, CH_3–N); 2.9 s ((6H, $(CH_3)_2$N–); 3.3 t (2H, –CH_2–N–); 3.85 t (2H, –CH_2–O–); 6.75–6.9 m (4H, –C_6H_4–).

N-(*4′-Dimethylaminophenyl*)-N-*methyladipic acid monoamide monoethyl ester, TriMPD-Ad* (**9**). 100 g adipic acid monomethyl ester were cooled with ice, and 100 g oxalyl chloride slowly added with exclusion of moisture. The mixture was reacted at room temperature for 3 days. Residual oxalyl chloride was removed *in vacuo*, and the remaining yellow oil of adipic acid monomethyl ester monochloride used without further purification. Then 94.9 g TriMPD (**3**) and 50 g pyridine were dissolved in THF, and cooled with ice. A solution of the crude adipic acid monomethyl ester monochloride in 200 ml THF was slowly added at room temperature, resulting in a strong exotherm. After stirring at room temperature for 16 h the mixture was filtered from the precipitated pyridine hydrochloride and the filtrate passed through a short column of basic Al_2O_3 and the solvent evaporated to yield 157 g (85%) of brown oil, which solidified upon cooling; $n_D^{22} = 1.5411$. High-resolution mass spectrum: signal at mass 292.1766; calculated for $C_{16}H_{24}N_2O_3$, 292.1787. ^{1}H n.m.r. (solvent $CDCl_3$), δ (ppm): 1.5–1.65 m (4H, –CH_2–CH_2–); 2.1 t (2H, –CH_2–COO–); 2.25 t (2H, –CH_2–CON–); 3.0 s (6H, $CH_3)_2$N–); 3.23 s (3H, CH_3–NCO–); 3.65 s (3H, CH_3–O–); 6.75 d (2H, N–C_6H_4–NCO–); 7.05 d (2H, –CON–C_6H_4–N).

N-(*4′-Dimethylaminophenyl*)-N-*methyl-6-aminohexanol, T6OH* (**10**). 157 g TriMPD-Ad (**9**) in 600 ml THF were reacted with 30 g $LiAlH_4$ suspended in 700 ml THF as described for TriMPD (**3**) above. The combined filtrates were evaporated to yield 122 g (90%) of a slightly yellow oil; $n_D^{22} = 1.5503$. High-resolution mass spectrum (trimethylsilyl derivative): signal at mass 322.2430; calculated

for $C_{18}H_{34}N_2OSi$, 322.2440. ^1H n.m.r. (solvent $CDCl_3$), δ (ppm): 1.3–1.4 m (4H, $-CH_2-CH_2-$); 1.5–1.6 m (8H, $-CH_2-CH_2-CH_2-CH_2-$); 2.84 s (9H, $(CH_3)_2N-$, CH_3-N-); 3.18 t (2H, $-CH_2-N-$); 3.65 t (2H, $-CH_2-O-$); 6.7–6.8 m (4H, $-C_6H_4-$).

N-(*4'-Dimethylaminophenyl*)-N-*methyl-2-aminoethyl methacrylate, T2M* (**11**). A mixture of 16.9 g T2OH (**7**) and 7.3 g pyridine in 100 ml THF was slowly added to 9.55 g methacryloyl chloride dissolved in 150 ml THF at room temperature. The mixture became milky, and a precipitate of pyridine hydrochloride was formed. After stirring for 72 h the mixture was filtered and the filtrate passed several times over short columns of basic Al_2O_3, until the solution was decolourized, and no more starting material could be detected by t.l.c. The solvent was evaporated at high vacuum for 2 days to yield 10.5 g (46%) of slightly yellow oil. High-resolution mass spectrum: signal at mass 262.1671; calculated for $C_{15}H_{22}N_2O_2$, 262.1681. ^1H n.m.r. (solvent $CDCl_3$), δ (ppm): 1.9 s (3H, $CH_3-C=$); 2.9 s (6H, $(CH_3)_2-N-$); 2.98 s (3H, CH_3-N-); 3.55 t (2H, $-CH_2-N-$); 4.35 t (2H, $-CH_2-O-$); 5.6 s (1H, C=CH *trans* C=O); 6.13 s (1H, –C=CH *cis* C=O); 6.7–6.85 m (4H, $-C_6H_4-$).

N-(*4'-Dimethylaminophenyl*)-N-*methyl-3-aminopropyl methacrylate, T3M* (**12**). 18.6 g methacryloyl chloride, 35.5 g T3OH (**8**) and 15 ml pyridine were reacted in THF and purified as described for T2M (**11**). Yield, 19.3 g (41%); slightly yellow oil. High-resolution mass spectrum: signal at mass 276.1824; calculated for $C_{16}H_{24}N_2O_2$, 276.1838. ^1H n.m.r. (solvent $CDCl_3$), δ (ppm): 2.0 m (5H, $CH_3-C=$, $-CH_2-$); 2.9 s broad (9H, $(CH_3)_2-N-$, CH_3-N-); 3.37 t (2H, $-CH_2-N-$); 4.27 t (2H, $-CH_2-O-$); 5.65 s (1H, C=CH *trans* C=O); 6.18 s (1H, –C=CH *cis* C=O); 6.75–6.85 m (4H, $-C_6H_4-$).

N-(*4'-Dimethylaminopyhenyl*)-N-*methyl-6-aminohexyl methacrylate, T6M* (**13**). 10.5 g methacryloyl chloride, 25.0 g T6OH (**10**) and 8.0 g pyridine were reacted in THF and purified as described for T2M (**11**), to yield 10.9 g (34%) of slightly yellow oil. High-resolution mass spectrum: signal at mass 318.2247; calculated for $C_{19}H_{30}N_2O_2$, 318.2307. ^1H n.m.r. (solvent $CDCl_3$), δ (ppm): 1.3–1.7 m (8H, $-CH_2-CH_2-CH_2-CH_2-$); 1.95 s (3H, $CH_3-C=$); 2.9 s (9H, $(CH_3)_2-N-$, CH_3-N-); 3.3 t (2H, $-CH_2-N-$); 4.15 t (2H, $-CH_2-O-$); 5.55 s (1H, C=CH *trans* C=O); 6.1 s (1H, –C=CH *cis* C=O); 6.75–6.85 m (4H, $-C_6H_4-$).

N-(*4'-Dimethylaminophenyl*)-N-*methyl-2-aminoethyl sorbate, T2S* (**14**). 43.2 g sorbyl chloride, 51 g T2OH (**7**) and 22 ml pyridine were reacted in THF and purified as described for T2M (**11**) to yield 19.3 g (25%) of slightly yellow-range oil. High-resolution mass spectrum: signal at mass 288.1840; calculated for $C_{17}H_{24}N_2O_2$, 288.1838. ^1H n.m.r. (solvent $CDCl_3$), δ (ppm): 1.9 m (3H, $CH_3-C=$); 2.88 s (6H, $(CH_3)_2-N-$); 2.95 s (3H, CH_3-N-); 3.5–3.7 m (2H, $-CH_2-N-$); 4.38 m (2H, $-CH_2-O-$); 5.8 m (1H, =CH–C); 6.2 m (2H, –CO–CH=C–CH=); 6.8 m (4H, $-C_6H_4-$); 7.25 m (1H, –CO–C=CH–).

N-(*4'-Dimethylaminophenyl*)-N-*methyl-3-aminopropyl sorbate, T3S* (**15**). 19.3 g sorbyl chloride, 29.2 g T3OH (**8**) and 12 ml pyridine were reacted in THF and purified as described for T2M (**11**). Yield, 11.6 g (27%); slightly yellow-orange oil. High-resolution mass spectrum: signal at mass 302.1997; calculated for $C_{18}H_{26}N_2O_2$, 302.1994. ^1H n.m.r. (solvent $CDCl_3$), δ (ppm): 1.95 m (5H, $CH_3-C=$, $-CH_2-$); 2.90 m (9H, $(CH_3)_2-N-$, CH_3-N-); 3.40 t (2H, $-CH_2-N-$); 4.30 t (2H, $-CH_2-O-$); 5.85 m (1H, =CH–C); 6.25 m (2H, –CO–CH=C–CH=); 6.8 m (4H, $-C_6H_4-$); 7.35 m (1H, –CO–C=CH–).

N-(*4'-Dimethylaminophenyl*)-N-*methyl-6-aminohexyl sorbate, T6S* (**16**). 13.1 g sorbyl chloride, 25.0 g T6OH (**10**) and 8.0 g pyridine were reacted in THF and purified as described for T2M (**11**), to yield 13.1 g (38%) of slightly yellow oil. High-resolution mass spectrum: signal at mass 344.2460; calculated for $C_{21}H_{32}N_2O_2$, 344.2464. ^1H n.m.r. (solvent $CDCl_3$), δ (ppm): 1.3–1.7 m (8H, $-CH_2-CH_2-CH_2-CH_2-$); 1.55 d (3H, $CH_3-C=$); 2.9 s (9H, $(CH_3)_2-N-$, CH_3-N-); 3.18 t (2H, $-CH_2-N-$); 4.12 t (2H, $-CH_2-O-$); 5.75 s (1H, =CH–C); 6.15 m (2H, –CO–CH=C–CH=); 6.8 m (4H, $-C_6H_4-$); 7.25 m (1H, –CO–C=CH–).

Synthesis of polymers

Homopolymers. Homopolymers of monomers (**11**)–(**16**) were prepared by group-transfer polymerization (GPT)[11–14] in THF, using 1-methoxy-1-trimethylsiloxy-2-methylprop-1-ene (MTS) as initiator system and 0.1 N THF solution of tetrabutylammonium bibenzoate (TBBiB) as catalyst[12]. Random copolymers and block copolymers of (**11**) and (**13**) with methyl methacrylate (MMA) were prepared by GTP as well. Typical procedures for homo- and copolymerization are given below for P-T2M (**17**), P-MMA/T2M-3 (**23**) and P-MMA/T2M-b15 (**27**). All procedures are summarized later in *Table 3*.

Poly[N-(*4'-dimethylaminophenyl*)-N-*methyl-2-amino ethyl methacrylate*], *P-T2M* (**17**). In a dry box, 2 g T2M (**11**) were dissolved in 6 ml THF. Then with stirring 50 μl of 1-methoxy-1-trimethylsiloxy-2-methylprop-1-ene (MTS) were added at 30°C, followed by 52 μl of a 0.1 N solution of tetrabutylammonium bibenzoate (TBBiB) in THF. The temperature of the mixture rises to 37°C within 2 min, and then cools down slowly. After stirring for 45 min the mixture was poured into 65 ml hexane and the precipitate isolated, washed with hexane and dried in vacuum to yield 1.7 g of colourless powder. Elemental analysis: C 67.30%, H 8.48%, N 9.69%; calculated for $C_{15}H_{22}N_2O_2$; C 68.70%, H 8.40%, N 10.67%.

Poly[*methyl methacrylate*-co-N-(*4'-dimethylamino-phenyl*)-N-*methyl-2-aminoethyl methacrylate*], *P-MMA/T2M-3* (**23**). 10 μl 1-methoxy-1-trimethylsiloxy-2-methyl-prop-1-ene (MTS) and 10 μl of a 0.1 N solution of tetra-butylammonium bibenzoate (TBBiB) in THF were dissolved in 3 ml THF at 29°C. A mixture of 1.1 g methyl methacrylate (MMA) and 0.9 g T2M (**11**) in 3 ml THF was added slowly, so that the temperature of the mixture stays below 45°C. After stirring for 90 min, the mixture was poured into 50 ml ether, the precipitate isolated, washed and dried in vacuum to yield 1.6 g of colourless powder. Elemental analysis: C 64.44%, H 8.87%, N 4.67%.

Poly[*methyl methacrylate*-block-N-(*4'-dimethylamino-phenyl*)-N-*methyl-2-aminoethyl methacrylate*], *P-MMA/T2M-b15* (**27**). 50 μl 1-methoxy-1-trimethylsiloxy-2-methyl-prop-1-ene (MTS) and 52 μl of a 0.1 N solution

of tetrabutylammonium bibenzoate (TBBiB) in THF were dissolved in 16 ml THF at 29°C. 5.1 g methyl methacrylate (MMA) are added slowly, keeping the reaction temperature below 55°C. When the addition of MMA was finished, and the temperature of the reaction mixture started to decrease, 2.0 g T2M (**11**) in 4 ml TMF were added. (Before the addition of (**11**), 1 ml of the reaction mixture was removed, precipitated into 5 ml ether, and isolated, to characterize the PMMA block.) After stirring for 90 min, the mixture was poured into 120 ml ether, the precipitate isolated, washed and dried in vacuum to yield 6.1 g of colourless powder. Elemental analysis: C 61.87%, H 8.90%, N 1.50%.

PMMA block: 0.13 g colourless powder. Elemental analysis: C 60.46%, H 8.25%; calculated for $C_5H_8O_2$: C 60.00%, H 8.00%.

Poly[N-(*4'-dimethylaminophenyl*)-*1-aza-3,4-dihydroxypentane*], *P-DMPA4* (**29**). 11.14 g 4-dimethylaminoaniline and 7.04 g butadiene diepoxide were added 100 ml THF, upon which the flask became cold. After stirring for 3 days the solution was heated at reflux for 3 h, and was then cooled to room temperature and stirred an additional 12 h. The orange solution was treated with 1 l of diethyl ether, resulting in precipitation of an orange powder. The powder was washed with diethyl ether and dried *in vacuo*. Yield: 12.1 g (67%). Elemental analysis: C 65.11%, H 8.16%, N 9.69%; calculated for $C_{11}H_{16}N_2O_2$: C 64.86%, H 8.11%, N 12.61%. I.r. (KBr, in cm^{-1}): 3100–2830 m, 2790 m, 1618 w, 1518 vs, 1475 m, 1455 m, 1445 m, 1322 m, 1302 m, 1260 m, 1220 m, 1160 m, 1135 m-s, 1095 s, 1060 m, 945 m, 816 m-s.

Poly[N-(*4'-dimethylaminophenyl*)-*1-aza-3,4-dihydroxynonane*], *P-DMPD8* (**30**). 8.87 g 4-dimethylaminoaniline and 9.27 g octadiene-1,2,7,8-diepoxide were mixed and stirred at room temperature for 3 days. The liquid was heated for another 22 h at 100°C to yield a yellow-orange, mostly insoluble glass. Yield: quantitative. Elemental analysis: C 68.69%, H 9.61%, N 12.20%; calculated for $C_{16}H_{26}N_2O_2$: C 64.86%, H 8.11%, N 12.61%. I.r. (KBr, in cm^{-1}): 3100–3000 w, 2980–2820 s, 2790 m, 1720 w, 1611 w-m, 1506 vs, 1472 m, 1453 m, 1442 m, 1323 m, 1225 m, 1208 m, 1185 m, 1165 m, 1080 s, 1060 s, 945 m, 816 m.

Poly[N-(*4'-dimethylaminophenyl*)-*1-aza-5,10-dioxa-3,12-dihydroxytridecane*], *P-DMPD12* (**31**). 9.94 g 4-dimethylaminoaniline and 14.76 g butadendiol diglycidyl ether are refluxed in 20 ml THF for 4 days. The viscous oil is precipitated into 500 ml ether. The precipitate is collected, washed and dried in vacuum. Yield: 18.9 g brownish, insoluble gum. Elemental analysis: C 63.90%, H 8.88%, N 18.28%; calculated for $C_{18}H_{30}N_2O_4$: C 63.32%, H 8.87%, N, 6.80%. I.r. (neat, in cm^{-1}): 3100–3000 vw, 2980–2820 s, 2790 m, 1745 w, 1611 w-m, 1513 v, 1475 m, 1450 m, 1440 m, 1320 s, 1220 s, 1185 w, 1165 w, 1095 s, 1045 vs, 980 s, 910 w, 810 s.

Poly[*ethylene*-co-N-(*4-dimethylaminophenyl*)*maleimide*], *P-Et/DPMI* (**32**). 20 g of ethylene maleic anhydride copolymer (Aldrich) and 21.9 g 4-dimethylaminoaniline were heated to reflux in 300 ml pyridine under nitrogen for 5 h. The 9.5 g sodium acetate and 100 ml acetic anhydride were added, and the mixture heated to reflux for an additional 16 h. The solution was cooled and poured into 4 ml of methanol. The resulting precipitate was washed with methanol and dried in vacuum at 40°C to yield 33.6 g (87%) of colourless powder. Elemental analysis: C 67.11%, H 6.36%, N 9.70%, O 15.86%; calculated for $C_{14}H_{16}N_2O_3$: C 68.85%, H 6.56%, N 11.48%, O 13.11%. I.r. (KBr, in cm^{-1}): 3100–2830 w, 2805 w, 1775 w, 1708 vs, 1612 m, 1522 s, 1446 w-m, 1390 m, 1353 m-s, 1185 m-s, 1170 m-s, 1063 w, 948 w, 815 w.

Poly[*ethylene*-co-N-(*4-dimethylaminophenyl*)*pyrroline*], *P-Et/DMPD* (**33**). 1 g $LiAlH_4$ was added cautiously under cooling to 50 ml freshly distilled, dry pyridine. After warming to room temperature, 4.9 g P-Et/DPMI (**32**) in 50 ml pyridine was slowly added. After stirring for 1 h and heating to reflux for 3 h, the mixture converted into a slurry. This was cooled with ice, 1.2 g ethyl acetate was added slowly followed by 2 g water. After centrifugation to remove the finely dispersed solids, the supernatant was poured into 600 ml ether, and the resulting precipitate isolated and dried in vacuum to yield 0.5 g of slightly brownish insoluble powder, which was discarded (elemental analysis: C 58.38%, H 7.01%, N 8.78%, ash observed).

The centrifugate was extracted for 3 days in a Soxhlet extractor with chloroform. The extract was poured into 600 ml ether, and the resulting precipitate isolated and dried. Yield: 0.2 g of brown, soluble powder. Elemental analysis: C 66.77%, H 7.41%, N 9.38%; calculated for $C_{14}H_{20}N_2$: C 77.78%, H 9.26%, N 12.96%. I.r. (cast, in cm^{-1}): 3100–2820 s, 2790 m, 1770 vw, 1680 m-s, 1612 m, 1573 w, 1519 vs, 1480 m, 1450 m, 1442 m, 1350 m, 1320 m-s, 1215 w, 1190 w, 1162 w, 1138 w, 1058 w, 1022 w, 945 m, 811 m, 750 s.

Poly[*methyl vinyl ether*-co-N-(*4-dimethylaminophenyl*)*maleimide*], *P-MVE/DPMI* (**34**). 15.6 g methyl vinyl ether maleic anhydride copolymer (Polysciences, $M_n = 41\,000$) and 13.7 g 4-dimethylaminoaniline were heated to reflux in 300 ml THF under nitrogen for 16 h. The mixture was poured into 8 l of methanol to precipitate 28.2 g of the amide acid polymer. Then 22 g of the amide acid polymer, 10.6 g sodium acetate and 100 ml acetic anhydride in 400 ml pyridine were heated to reflux for an additional 3 h. The cooled solution was poured into 4 l of methanol, the precipitate collected, washed with methanol and dried in vacuum. Yield: 19.5 g of brownish powder. Elemental analysis: C 65.28%, H 6.33%, N 9.68%, O 18.69%; calculated for $C_{15}H_{18}N_2O_3$: C 65.69%, H 6.57%, N 10.22%, O 17.52%. I.r. (KBr, in cm^{-1}): 3100–2820 w, 2800 w, 1770 w, 1708 vs, 1611 m, 1522 s, 1445 w, 1392 w, 1352 m, 1188 m, 1165 m, 1100 w-m, 945 w, 812 w.

Poly[*methyl vinyl ether*-co-N-(*4-dimethylaminophenyl*)*pyrroline*], *P-MVE/DMPD* (**35**). 1 g $LiAlH_4$ was added cautiously under cooling to 50 ml freshly distilled dry pyridine. After warming to room temperature, 5.0 g P-MVE/DPMI (**34**) in 100 ml pyridine were slowly added. After stirring for 1 h, and heating to reflux for 3 h, the mixture converted into a gel. This was cooled with ice and 4 g ethyl acetate added slowly, followed by 2 g water. After centrifugation the precipitate was saved and the supernatant was poured into 500 ml of ether, and the precipitate isolated. Both precipitates were combined and extracted for 60 h with chloroform in a Soxhlet extractor. The extract was poured into 500 ml ether and the precipitate isolated and dried in vacuum at 50°C to yield

0.8 g of brownish powder. Elemental analysis: C 69.04%, H 7.47%, N 11.08%; calculated for $C_{15}H_{22}N_2O$: C 73.17%, H 8.94%, N 11.38%. I.r. (cast, in cm^{-1}): 3100–2820 m-s, 2795 m, 1760 vw, 1690 m-s, 1612 m, 1510 vs, 1480 m, 1455 m, 1443 m, 1350 m-s, 1320 m-s, 1217 w, 1190 w, 1164 w, 1135 w, 1095 w, 1060 w, 945 m, 812 m-s.

Methods

I.r. spectra were taken with a Nicolet 60SX instrument. U.v./vis./n.i.r. spectra were recorded with a Varian Cary 2300 spectrophotometer. N.m.r. spectra were recorded with a General Electric QE-300 instrument. Elemental analysis was performed by Micro-Analysis, Wilmington. Thermal characterizations were performed by a Du Pont Instruments 951 Thermogravimetric Analyzer and a Du Pont Instruments 912 Differential Scanning Calorimeter. High-resolution mass spectra were measured by a Micromass 7070HS, VG-Organic Ltd.

Cyclic voltammetry was performed at room temperature in a nitrogen atmosphere, with a Princeton Applied Research model 273 potentiostat, in acetonitrile and dichloromethane containing 0.1 M tetrabutylammonium perchlorate (TBAP). Platinum electrodes were used for working and counter electrodes, and a Ag/AgCl electrode (Ag/AgCl) as a reference electrode.

The experimental apparatus for quartz crystals microbalance (QCM) investigations comprised a 0.5 inch diameter 6 MHz AT-cut quartz crystal and a home-made oscillator designed to drive the crystal at its resonant frequency. Gold electrodes (2000 Å thick) were deposited on chromium underlayers (200 Å) on both sides of the crystal using evaporative techniques. The patterns were arranged so that the gold leads from the outer edges of the crystal to the centre circular pad on opposite sides did not overlap. The sensitivity of the QCM is 12.28 ng Hz^{-1} cm^{-2}. The frequency of the QCM was monitored with a Hewlett Packard 5384A frequency counter and recorded with a Digital Equipment Corp. PDP-11/73 computer, as described previously[30]. The active area of the piezoelectric crystal was coated with polymer by addition with a microlitre syringe of aliquots of known concentration.

Oxidation in solution was accomplished by dissolving 0.1–1 mmol polymer in 5 ml dichloromethane followed by addition of the calculated amount of oxidant, depending on the desired extent of oxidation. The mixture was allowed to react for 15 min, and was then poured into 100 ml hexane. The resulting precipitate was isolated and dried and pressed into pellets as described above.

For oxidation and complexation of polymers with electron acceptors, ~0.2 mmol polymer were dissolved in 2 ml dichloromethane, and a solution/suspension of the calculated amount of electron acceptor in 5 ml dichloromethane added. The mixture was reacted overnight and precipitation completed by addition of 10 ml hexane. The precipitates were isolated and dried. Polymer oxidation in bulk was performed by exposing pellets prepared by applying 5000 psi pressure to the polymers to vapours of the oxidant in an air-filled flask.

D.c. conductivity experiments were performed as two-probe measurements on platinum electrodes by measuring resistance with either a Keithley 616 Digital Electrometer (for $R > 10^7\ \Omega$ cm) or a Keithley 177 Microvolt DMM. The limit of sensitivity was $20 \times 10^{12}\ \Omega$. Unless noted otherwise, all resistances were measured at $22 + 1$°C. The conductivity was considered to be electronic if the resistivity stayed constant over several minutes and did not drop on reversing the polarity. Otherwise, the conductivity was considered to have an ionic contribution. Conductivities were measured during doping using pellets prepared by applying 5000 psi pressure to the polymers. The pellets were cut into rectangular 4 mm × 0.2 mm × 0.2 mm bars, which were then attached to platinum electrodes by conductive paste (Acheson, Electrodag + 502, graphite in methyl ethyl ketone). The sample was placed in an air-filled flask at 22°C containing ~2 g iodine crystals. The thermal dependence of conductivity of P-T2M (**17**) was measured with a four-probe method by fixing the rectangular bar to platinum wires with Electrodag + 502 conductive paste. The sample was exposed to vacuum (10^{-4} Torr) for 15 min, and then exposed to helium for measurement.

RESULTS AND DISCUSSION

Polymer structures and molecular weights

The polymers synthesized and the corresponding monomers and model compounds investigated are shown in *Tables 1* and *2*, and their basic properties listed in *Tables 3–5*.

Polymers with phenylenediamine moieties in the polymer side-chain were synthesized by group-transfer polymerization (GTP)[11–14]. Homopolymers (**17**)–(**22**) of the methacrylate and sorbate monomers (**11**)–(**16**) and copolymers with methyl methacrylate (MMA) (**23**)–(**28**) were synthesized using a silyl ketene acetal initiator/oxyanion catalyst system[12]. The polymerization parameters are summarized in *Table 3*, and the copolymer

Table 1 Molecular structures of TMPD monomers and model compounds

Compound		Structure	*n*	R
1	DMPD			
4	TMPD	II		
5	TMSt	III		
6	TMAzo	IV		
7	T2OH	V	2	OH
8	T3OH	V	3	OH
10	T6OH	V	6	OH
11	T2M	V	2	OOC–C(CH_3)=CH_2
12	T3M	V	3	OOC–C(CH_3)=CH_2
13	T6M	V	6	OOC–C(CH_3)=CH_2
14	T2S	V	2	OOC–CH=CH–CH=CH–CH_3
15	T3S	V	3	OOC–CH=CH–CH=CH–CH_3
16	T6S	V	6	OOC–CH=CH–CH=CH–CH_3

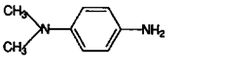

I

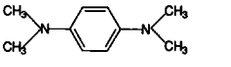

II

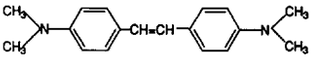

III

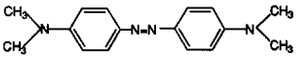

IV

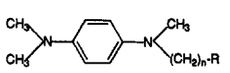

V

compositions in *Table 4*. The molecular weights of the polymers obtained are listed in *Table 5*. Characteristically, most molecular-weight distributions show tailing or bimodality, with fractions of molecular weight well above 100 000. The amounts of initiator used should produce molecular weights of 10 000–20 000, however, assuming living polymerization[11]. Most probably, this is caused by traces of impurities, which could not be removed from the monomers, resulting in premature termination of some growing polymer chains. Nevertheless, the high yields of polymer obtained demonstrate that the polymerization processes are able to tolerate impurities.

Table 2 Molecular structure of TMPD polymers

Polymer	Structure	*n*	R
17 P-T2M	I	2	
18 P-T3M	I	3	
19 P-T6M	I	6	
20 P-T2S	II	2	
21 P-T3S	II	3	
22 P-T6S	II	6	
29 P-DMPD4	III		–
30 P-DMPD8	III		$(CH_2)_4$
31 P-DMPD12	III		CH_2–O–$(CH_2)_4$–O–CH_2
33 P-Et/DMPD	IV		H
34 P-MVE/DMPD	IV		O–CH_3

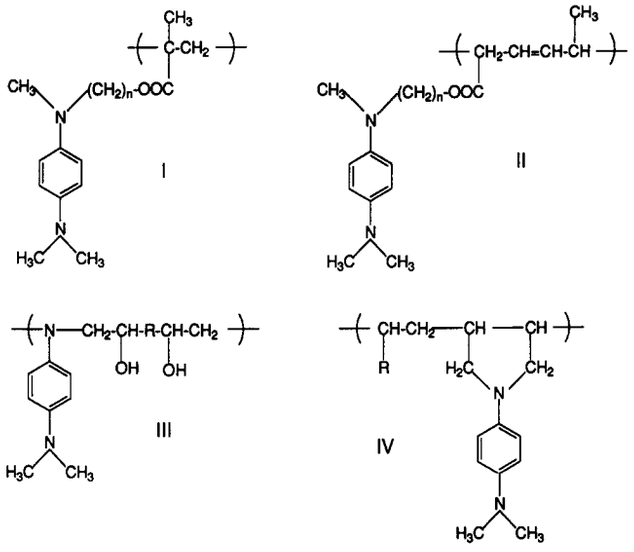

Because the additional methylene groups in polymers P-T2M, P-T3M and P-T6M (**17**)–(**19**) partially overlap the ^{1}H n.m.r. signals of the methyl group (*Figure 1*), tacticities of the polymers could not be determined exactly. The approximate amounts of tacticity for all polymers were ≤5% isotactic, 35–40% heteroatactic and 55–60% syndiotactic methyl groups, being close to the reported tacticities of PMMA prepared by GTP at 30°C[13]. In the poly(sorbates) (**20**)–(**22**), the polymerization of the butadiene moiety takes place at the 1,4-position[14], as shown by the ^{1}H n.m.r. spectra (*Figure 2*). The signal at $\delta = 5.4$ ppm indicates the formation of an isolated C)C double bond, and the signal at $\delta = 0.95$ ppm indicates the presence of a methyl group next to a saturated C atom. The i.r. band at 970 cm^{-1} points to predominant *trans* double bonds in the backbone, in agreement with detailed ^{13}C n.m.r. of poly(ethyl sorbate) prepared by GTP[14]. In contrast to GTP, radical polymerization of monomers (**17**)–(**22**) was not successful. Attempts to polymerize the methacrylates with AIBN yielded insoluble polymers only, with low glass transition temperatures compared to polymers prepared by GTP. Obviously, side-reactions presumably linked to the phenylenediamine moieties cause fast termination and crosslinking of the growing polymer chains. Radical polymerization of the sorbates failed too, yielding low oligomers only. The successful polymerization of these monomers achieved by GTP exemplifies the potential of this technique for speciality polymer synthesis. Functional groups, which are sensitive to the 'classical'

Table 3 GTP of monomers (**11**)–(**16**) on THF, homopolymers and copolymers with MMA

Polymer	Monomer	Feed (g)	MMA (g)	MTS (μl)	0.1N TBBiB (μl)	Yield (g)
Homopolymers						
P-T2M (**17a**)	T2M	2.0	–	50	52	1.7
(**17b**)		1.5	–	20	50	
(**17c**)		1.8	–	20	50	
P-T3M (**18a**)	T3M	1.0	–	15	30	
(**18b**)		0.6	–	110	75	
P-T6M (**19a**)	T6M	2.1	–	40	42	1.7
(**19b**)		0.43	–	7	20	
P-T2S (**20a**)	T2S	2.1	–	20	100	1.8
(**20b**)		1.5	–	20	100	
P-T3S (**21a**)	T3S	1.7	–	30	30	1.7
(**21b**)		3.6	–	70	150	
P-T6S (**22a**)	T6S	2.1	–	40	42	2.0
Random copolymers						
P-MMA/T2M-3 (**23**)	T2M	0.9	1.1	10	10	1.6
P-MMA/T2M-7 (**24**)	T2M	2.2	5.3	50	52	6.6
P-MMA/T6M-4 (**25**)	T6M	1.9	1.9	18	58	2.9
P-MMA/T6M-7 (**26**)	T6M	1.3	2.6	25	50	3.7
Block copolymers						
P-MMA/T2M-b15 (**27**)	T2M	2.2	5.3	50	52	6.6
P-MMA/T6M-b7 (**28**)	T6M	1.9	1.9	18	58	2.9

Table 4 Composition of copolymers prepared from T2M (**11**) and T6M (**13**). Mole fraction of methyl methacrylate x_{MMA} in the monomer feeds and in the polymers

Copolymer	Monomer feed, x_{MMA}	Polymer content x_{MMA}	
		by elemental analysis	by ^{1}H n.m.r.
P-MMA/T2M-3 (**23**)	0.75	0.77	0.76
P-MMA/T2M-7 (**24**)	0.75	0.77	0.76
P-MMA/T6M-4 (**25**)	0.75	0.77	0.76
P-MMA/T6M-7 (**26**)	0.75	0.77	0.76
P-MMA/T2M-b15 (**27**)	0.75	0.77	0.76
P-MMA/T6M-b7 (**28**)	0.75	0.77	0.76

Table 5 Thermal stabilities, glass temperatures T_g and molecular weights of the polymers synthesized

Polymer	T_g by d.s.c. (°C)	Molecular weight		Method[a]
		M_n	M_w	
P-DMPD4	72	1 100		V.p.o.
P-DMPD8	72			i
P-DMPD12	31			i
P-Et/DPMI	195	6 150		V.p.o.
P-MVE/DPMI	221	9 120		V.p.o.
P-MVE/DMPD		1 150	2 360	G.p.c.(PS)
P-T2M **a**	43	18 300	104 000	G.p.c.(PS) b
b	41	12 600	148 000	G.p.c.(PS) b
c	39	45 100	194 000	G.p.c.(PS) b
P-T3M **a**	25	12 500	34 800	G.p.c.(PS) t
b	0	2 450	6 650	G.p.c.(PS) b
P-T6M **a**	5	8 750	17 800	G.p.c.(PS) t
		8 440		V.p.o.
b	12	16 400	20 500	G.p.c.(PS)
P-T2S **a**	20	13 300	38 700	G.p.c.(PS) t
b	21	20 700	47 600	G.p.c.(PS) t
P-T3S **a**	10	21 900	37 300	G.p.c.(PS) t
b	13	44 000	83 000	G.p.c.(PS) t
P-T6S **a**	2			
P-MMA/T2M-3	89	15 400	30 000	G.p.c.(PMMA) t
P-MMA/T2M-7	104	13 200	43 800	G.p.c.(PMMA) t
P-MMA/T6M-4	70	17 600	871 000	G.p.c.(PMMA) b
P-MMA/T6M-7	88	29 700	697 000	G.p.c.(PMMA) b
P-MMA/T2M-b15	115	34 200	44 400	G.p.c.(PMMA)
PMMA block	125	31 300	44 300	G.p.c.(PMMA)
P-MMA/T6M-b7	111	20 800	321 000	G.p.c.(PMMA) b
PMMA block	120	14 500	17 400	G.p.c.(PMMA)

[a] Gel permeation chromatography, g.p.c.: b = bimodal distribution, t = shoulder/tailing; PS/PMMA = polystyrene standard/PMMA standard. Vapour pressure osmometry, v.p.o.

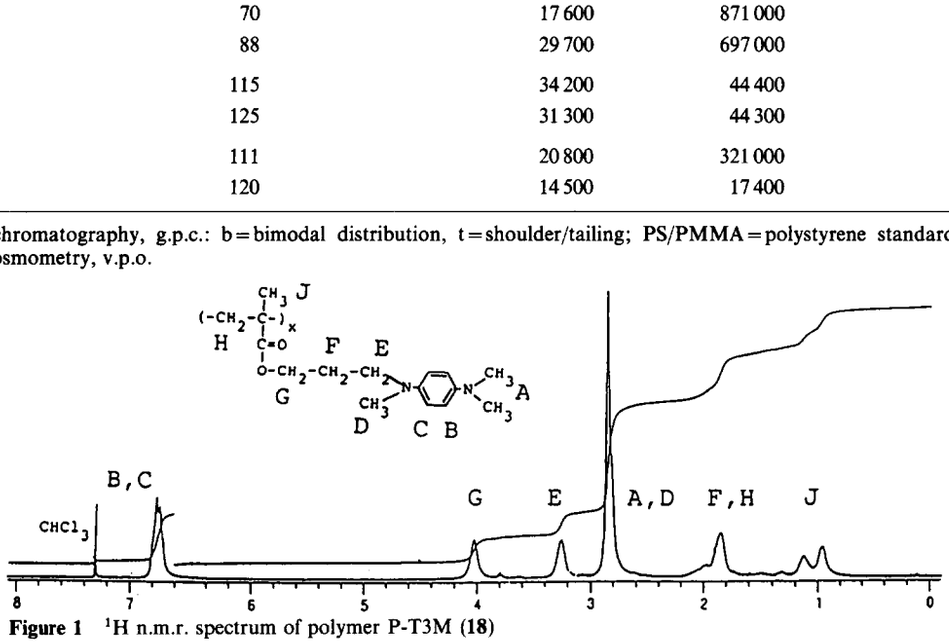

Figure 1 ^{1}H n.m.r. spectrum of polymer P-T3M (**18**)

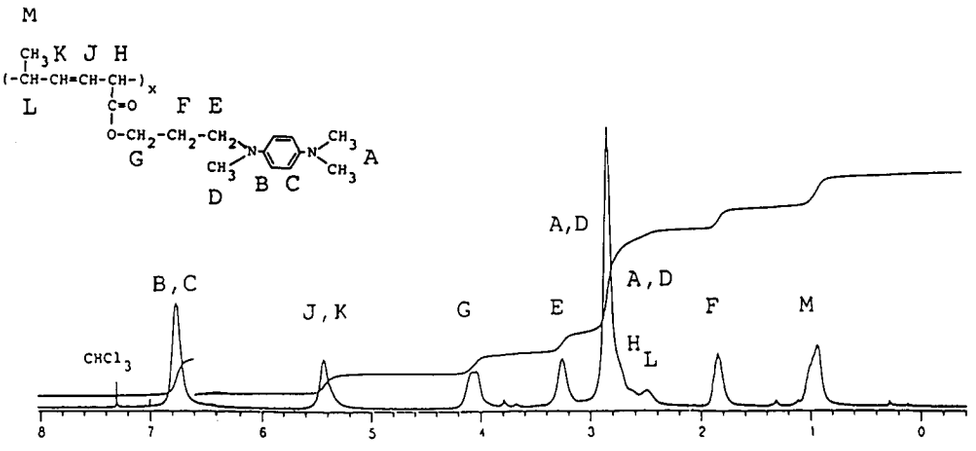

Figure 2 ^{1}H n.m.r. spectrum of polymer P-T3S (**21**)

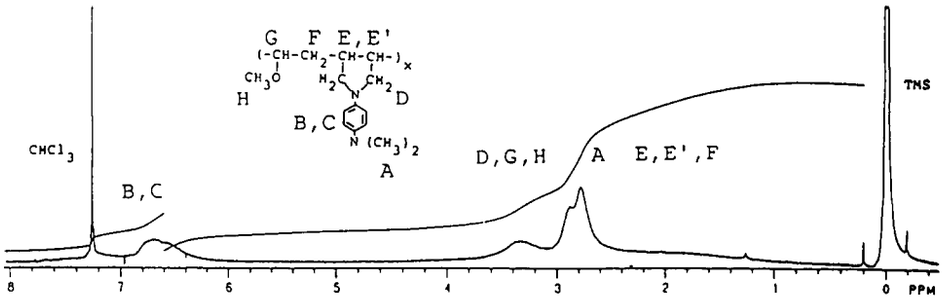

Figure 3 ^{1}H n.m.r. spectrum of polymer P-MVE/DMPD (**35**)

polymerization processes, are readily incorporated into homo- and copolymers.

To incorporate phenylenediamine moieties into a polymer backbone, other synthetic routes have to be chosen than GTP. Polymers (**29**)–(**31**) were prepared by reaction of *N*,*N*-dimethylaminoaniline with diepoxides[7,8]. This method yielded only soluble oligomers, or insoluble resins. This phenomenon is well known and attributed to crosslinking side-reactions of various types[7,8]. Polymers (**33**) and (**35**) were prepared by polymer analogue reactions, starting from maleic anhydride copolymers and *N*,*N*-dimethylaminoaniline. The resulting amide acids are cyclized to the imides, and subsequently reduced by $LiAlH_4$ in pyridine. This reduction of maleimide-containing polymers is very efficient insofar as ^{1}H n.m.r. shows signals of the aromatic protons of the phenylene-diamine moiety at 6.3–6.9 ppm only, but signals at 7.05 ppm pointing to residual imide groups are missing (*Figure 3*). In agreement, i.r. spectra exhibit nearly complete loss of the 1705–1710 cm^{-1} band of the imide moiety. However, the overall yields of polymers are low. It is assumed that the low yields are caused by strong absorption of phenylenediamine polymers on the Al_2O_3 formed in the reaction. This explanation agrees with the dramatic drop of molecular weights obtained (*Figure 5*), as high-molecular-weight polymers should be adsorbed preferentially, thus lowering the molecular weights of the products isolated.

The various polymers prepared enable examination of the role of concentration, aggregation and mobility on molecular properties such as oxidation potential. Polymers and oligomers (**29**)–(**31**), (**33**) and (**35**) represent type B polymers (*Scheme 1*). Whereas the phenylenediamine groups are most rigidly fixed in the backbones of polymers P-Et/DMPD (**33**) and P-MVE/DMPD (**35**) due to the pyrrolidine ring, they are more flexibly incorporated in the backbones in the case of the epoxide polymers (**29**)–(**31**), P-DMPD4, P-DMPD8 and P-DMPD12. The variation of the length of the flexible alkyl units gives polymers of analogous structure with different concentration and mobility of the redox-active functional group. Type C polymers (*Scheme 1*)) were derived from *N*-alkyl-*N*,*N*,*N*′-trimethyl-1,4-phenylenediamine. This moiety was bound to methacrylate or sorbate via ethyl, propyl and hexyl spacers. The various methacrylate and sorbate polymers enable examination of the role of concentration and mobility on molecular properties. The different lengths of the alkyl spacers modify the distance between backbone and functional group. Homologous polymethacrylates and polysorbates are distinguished by a different distance between subsequent functional groups, thus varying concentration and, possibly, aggregation behaviour. According to molecular models, two neighbouring phenylenediamines can aggregate in the polysorbates, but cannot aggregate in the polymethacrylates. In analogy, dilution and aggregation effects may be studied via the copolymers of MMA, T2M (**11**) and T6M (**13**).

Physical properties

Solubility. Except for the apparently crosslinked polymers, all the polymers synthesized are soluble in chloroform, dichloromethane, THF, DMF and pyridine. On prolonged storage periods in air, the polysorbates tended to cure, and to become insoluble. Nitrobenzene is an excellent solvent as well; however, the solutions are deeply brown coloured, suggesting formation of CT complexes with the phenylenediamine groups. Although

the polymers do not dissolve in water, solubility can be realized in HCl solutions due to protonation and conversion of the polymers into polyelectrolytes. Typical non-solvents for the polymers are acetone, acetonitrile, diethyl ether, hexane, isopropanol, methanol and toluene.

Thermal analysis. The thermal characteristics and the molecular weights of the polymers are listed in *Table 5*. The majority of the polymers are stable up to 200°C under nitrogen, as studied by thermogravimetry, generally decomposing between 200 and 300°C. Exceptions are the polymers P-Et/DMPD (**33**) and P-MVE/DMPD (**35**), which start to decompose between 110 and 150°C. Although there is no obvious reason for the thermal instability of these polymers, this behaviour may be due to the presence of functionalities that result from inadvertent reduction of the cyclic imide groups during synthesis, which gives rise to side-reactions, as evidenced by the weak absorption bands between 1700 and 1800 cm^{-1}.

As expected, the polymers with imide functionalities P-Et/DMPI (**32**) and P-MVE/DPMI (**34**) show the highest glass temperatures T_g in the series, in the range of 190–230°C. T_g of the maleimides rises with the bulkiness of the alternating comonomer: P-Et/DPMI < P-MVE/DPMI. In the series of polymers with DMPD in the backbone P-DMPD4 (**29**), P-DMPD8 (**30**) and P-DMPD12 (**31**), T_g decreases with increasing length of the alkyl spacer group. The polymethacrylates and polysorbates (**17**)–(**22**) prepared by GTP exhibit a decrease of T_g with increasing length of the alcohol units, in agreement with the well known decrease of T_g of poly(n-alkyl methacrylates) (*Table 5*). T_g of the polysorbates are lower than that of the homologous polymethacrylates. Except for P-T2M (**17**), the T_g values lie at or below room temperature. In the series of copolymers (**23**)–(**26**), T_g increases with the MMA content. Thus, functional polymers with T_g well above room temperature are obtained. In the cases of the block copolymers (**27**) and (**28**), only one glass transition is observed, with T_g values close to the one of PMMA.

Electrochemical properties

Cyclic voltammetry (c.v.) provides information about redox potentials of the parent compounds, as well as stability of the oxidized species. The various polymers synthesized, and several intermediates, were investigated by c.v. to establish a correlation between molecular structure and redox behaviour associated with phenylenediamine → semiquinone → quinodiimine transformations. The results of the c.v. studies in acetonitrile and in dichloromethane are summarized in *Tables 6* and *7*. Representative cyclic voltammograms of polymers are displayed in *Figures 4–6*.

Scheme 2

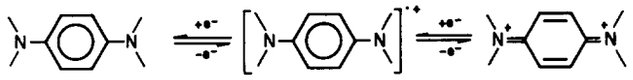

The electrochemical data presented in *Table 6* illustrate the importance of a rigid planar structure of the redox-active moiety. Although the π-electron system of TMSt (**5**) and TMAzo (**6**) are more extended compared to the various phenylenediamines, the oxidation potentials are higher. This can be rationalized by distorted planarity of the two aromatic cores. Thus, the effective resonance stabilization energy of the analogues to the semiquinone radical ion and to the quinonediimine respectively are reduced to the 1,4-phenylenediamine system. This observation agrees well with c.v. studies on 4,4'-diaminobiphenyl derivatives[15] and polyaminotriphenylenes[16]. In the case of the azo dye TMAzo (**6**), the slightly electron-withdrawing diazo moiety will also increase the oxidation potential. In addition to the effect of planarity, the data of *Tables 6* and *7* suggest that increasing *N*-alkylation lowers the redox potentials additionally[5].

Comparing TMPD (**4**) with the intermediates T2OH (**7**), T3OH (**8**), T6OH (**10**) and the methacrylates and

Table 6 Oxidation potentials of intermediates and monomers in dichloromethane and acetonitrile, Pt electrode, 0.1 M $(n\text{-}C_4H_9)_4N^+ClO_4^-$, sweep rate 0.1 V s^{-1}, in V vs. Ag/AgCl

Compound	E_{p,a_1}	E_{p,c_1}	E_{0_1}	ΔE_p	E_{p,a_2}	E_{p,c_2}	E_{0_2}	ΔE_p
Methylene chloride								
TriMPD	0.98	−0.11	0.44	1.09	–[a]			
TMPD	0.58	−0.02	0.28	0.60	0.93	0.73[a]	0.83	0.20
T2OH	0.55	−0.03	0.26	0.58	0.93	0.75[a]	0.84	0.18
T3OH	0.55	−0.07	0.24	0.62	0.90	0.72[a]	0.81	0.28
T6OH	0.78	−0.18	0.30	0.96	–[a]			
T2M	0.33	0.17	0.25	0.16	0.93	0.73[a]	0.83	0.20
T3M	0.34	0.20	0.27	0.14	0.97	–[a]		
T6M	0.46	0.10	0.28	0.36	1.13	0.76[a]	0.95	0.37
T2S	0.41	0.21	0.31	0.20	1.04	0.76[a]	0.90	0.28
T3S	0.37	0.18	0.28	0.19	1.00	0.79[a]	0.90	0.21
T6S	0.39	0.13	0.26	0.26	1.04	0.77[a]	0.91	0.27
Acetonitrile								
PD[b]	0.43	0.30	0.37	0.13	1.02	0.85	0.94	0.17
DMPD	0.33	0.23	0.28	0.10	0.91	0.81	0.86	0.10
TMPD	0.32	0.08	0.20	0.24	0.93	0.70	0.82	0.23
TMSt	0.53	0.42	0.48	0.11				
TMAzo	0.67	0.62	0.65	0.05				

[a] Not fully reversible, side-reactions occur
[b] PD = phenylenediamine

Table 7 Oxidation potentials of polymers in dichloromethane, Pt electrode, 0.1 M $(n\text{-}C_4H_9)_4N^+ClO_4^-$, sweep rate 0.1 V s^{-1}, in V vs. Ag/AgCl

Compound	E_{p,a_1}	E_{p,c_1}	E_{0_1}	ΔE_p	E_{p,a_2}	E_{p,c_2}	E_{0_2}	ΔE_p
P-T2M **a**	0.27	0.19	0.23	0.08	0.84	0.65[a]	0.75	0.19
P-T2M **b**	0.30	0.13	0.22	0.17	0.80	0.68[a]	0.74	0.12
P-T2M **c**	0.35	0.13	0.24	0.22	0.83	0.68[a]	0.76	0.15
P-T3M	0.32	0.19	0.26	0.13	0.81	0.65[a]	0.76	0.16
P-T6M	0.31	0.16	0.24	0.15	0.84	0.68[a]	0.76	0.16
P-T2S	0.32	0.14	0.23	0.18	0.80	0.63[a]	0.71	0.17
P-T3S	0.30	0.16	0.23	0.14	0.81	0.64[a]	0.73	0.17
P-MMA/T2M-3	0.35	0.23	0.29	0.12	1.00	0.83[a]	0.92	0.17
P-MMA/T2M-7	0.29	0.18	0.24	0.11	0.94	0.73[a]	0.84	0.21
P-MMA/T6M-4	0.25	0.20	0.23	0.05	0.88	0.75[a]	0.81	0.13
P-MMA/T6M-7	0.25	0.15	0.20	0.10	0.90	0.72[a]	0.81	0.18
P-MMA/T2M-b15	0.32	0.09	0.21	0.23	1.00	0.78[a]	0.89	0.22
P-MMA/T6M-b7	0.24	0.14	0.19	0.10	0.91	0.70[a]	0.81	0.21
P-DMPD4	0.36	0.09	0.23	0.27	0.87	0.58[a]	0.73	0.29
P-DMPD8	0.21	0.17	0.19	0.04	0.70	0.66[a]	0.68	0.04
P-DMPD12	0.27	0.20	0.24	0.07	0.75	0.70[a]	0.73	0.05
P-Et/DMPI	0.95	–[a]						
P-MVE/DMPI	1.3	–[a]						
P-Et/DMPD	0.22	0.16	0.19	0.06	–[a]			
P-MVE/DMPD	0.25	0.17	0.21	0.08	0.80[a]			

[a] Not reversible, side-reactions occur

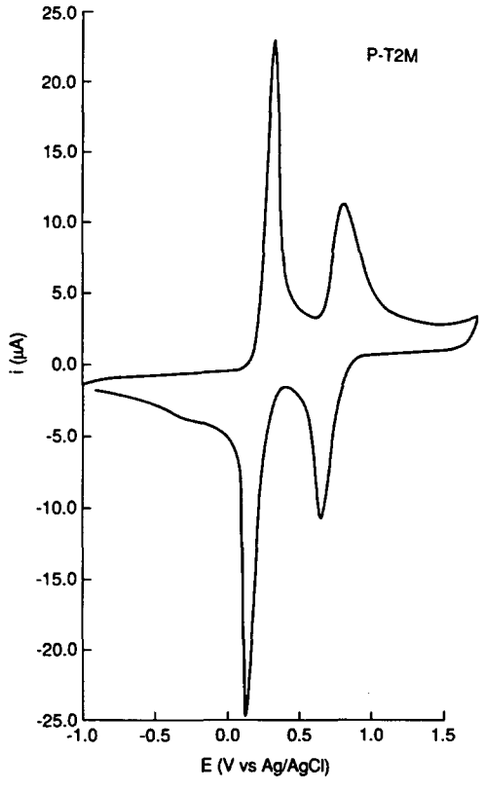

Figure 4 Cyclic voltammogram of P-T2M in 0.1 M TBAP/methylene chloride; $v = 100$ mV s^{-1}

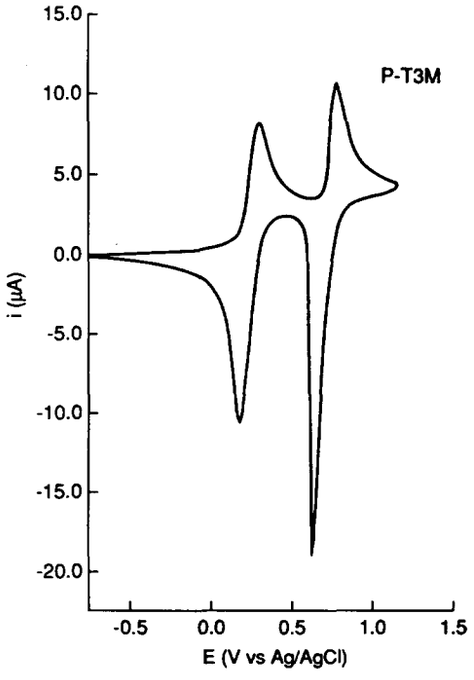

Figure 5 Cyclic voltammogram of P-T3M in 0.1 M TBAP/methylene chloride; $v = 100$ mV s^{-1}

sorbates (**11**)–(**16**), there is no significant difference in their redox potentials. Obviously, the oxidation potential is rather insensitive to secondary substitution effects away from the aromatic core. In contrast, considerable electronic and steric effects have been discussed for the effect of ring substitution on the oxidation potential of phenylenediamines[17]. Considering the influence of the solvent on the redox properties, the oxidation potentials of the first oxidation step in methylene chloride are slightly higher compared to acetonitrile solution. It should be noted that in acetonitrile both oxidation steps of the *N*-substituted phenylenediamines were electrochemically reversible. However, in methylene chloride only the first oxidation step to the semiquinone radical cation was reversible whereas the second oxidation step to the quinonediimine dication tended to be only partially reversible. The stability of the dication seems to improve

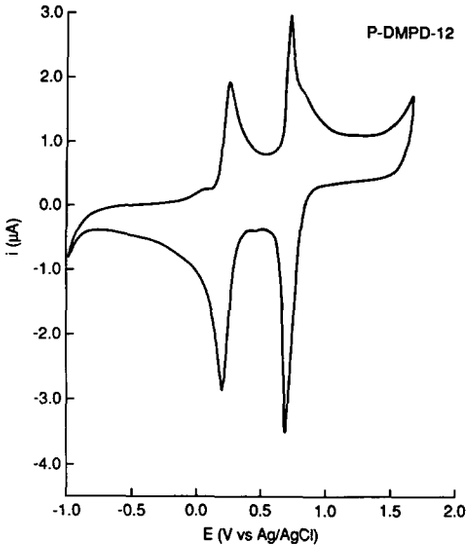

Figure 6 Cyclic voltammogram of P-DMPD-12 in 0.1 M TBAP/methylene chloride; $v = 100\,mV\,s^{-1}$

by subsitution of the methyl with increasingly hydrophobic residues. The first oxidation step of the model compounds TMSt (**5**) and TMAzo (**6**) are fully reversible as well. The large ΔE_p observed for TMPD (**4**) in 0.1 M TBAP is attributed to the decreased polarity of this medium as voltammograms recorded in 0.2 M TBAP exhibited smaller peak separations.

Incorporation of the phenylenediamine moiety into polymers did not modify the redox properties notably, as there was no significant difference in the redox potentials between the monomers and polymer compounds (*Tables 6* and *7*). Generally, the first oxidation step leading to the semiquinone is fully reversible. However, the polymers commonly formed films on the electrodes after the second oxidation, as suggested by the narrow shape of the voltammetric waves observed for the return cathodic waves and occasionally for the first oxidation step. On indium–tin oxide electrodes and platinum electrodes, the deposition is evident from the dark-blue films that were apparently not soluble in dichloromethane. However, the narrow waveshape is not solely attributed to classic adsorption waves due to surface-bound polymer. Indeed, in all cases the peak current was proportional to $v^{1/2}$, consistent with diffusion limitations. This may reflect diffusion limitations in the film itself due to low mobility of ionic charge carriers. It should be noted that the narrow waveshapes were most pronounced when the potential was cycled over both waves. When cycling was restricted to one of the waves, only diffusion shaped peaks were observed. The polymers do exhibit differences with regard to the pattern of the narrow waves. For example P-T3M shows a narrow wave for the cathodic branch of the 2+/1+ couple, whereas P-T2M exhibits narrow waves for both the anodic and cathodic branches of the 0/1+ couple, although the cathodic branch is generally more narrow. This may reflect reorganization phenomena in these films that depends upon the respective orientation of the redox-active groups. The narrow waveshape may also be indicative of interactions between redox-active groups in the polymer. For example, similar effects observed for polyvinylferrocene films in aqueous media were attributed to the presence of strong interactions between ferrocene sites and the presence of domains in the polymer[18]. For example, the narrow cathodic waves associated with reduction of P-T3M^{2+} may reflect the presence of attractive interactions between sites in P-T3M^{2+}.

N-Acylation leads to substantially increased oxidation potentials. The comparison of the analogues P-Et/DPMI and P-Et/DMPD or P-MVE/DPMI and P-MVE/DMPD, respectively, is most instructive. Furthermore, the oxidation process becomes irreversible, demonstrating the instability of *N*-acylated phenylenediamine radical ions.

It is noteworthy that different batches of P-T2M (**17a**, **b**, **c**; see *Table 5*) with different molecular weights show virtually identical redox potentials E_{0_1} (*Table 7*). The same is true for the various copolymers of MMA and T2M (**11**) or MMA and T6M (**13**) respectively, with no regard to composition or copolymer structure (random vs. block copolymers). Hence, even very different polymer structures bearing *N*,*N*,*N*′,*N*′-tetraalkyl-1,4-phenylenediamine groups do not affect the redox behaviour notably.

Cyclic voltammetry shows that the oxidation of polymers containing *N*,*N*,*N*′,*N*′-tetraalkyl-1,4-phenylenediamine leads to stable radical cations in solution. The oxidation potentials are so low that in addition to electrochemical oxidation the use of even weak oxidants can be considered. Although *N*-acylation affords precursor compounds with greater oxidative stability, it seems to be less desirable than *N*-alkylation as stronger oxidants are required and the oxidation step is irreversible.

Interaction with oxidants and electron acceptors

According to the low oxidation potentials, the polymers should be readily oxidized by electron acceptors to form charge-transfer (CT) complexes. Indeed, polymers in bulk or in solution are readily oxidized by 1 mol of iodine, bromine, hydrogen peroxide and chloranil, as indicated by the deep blue colour of the semiquinoid radical cations and their characteristic absorption bands in the visible[28,29] between 500 and 700 nm (*Figures 7* and *8*). Detailed studies were performed with polymer P-T2M (**17**). The reflection spectra obtained after addition of 1 mol of TCNE and TCNQ show, in addition to these bands, absorption tails up to 1700 nm indicative of CT interactions in the oxidized polymer. These absorptions are attributed to the formation of a TMPD radical cation–electron acceptor radical anion charge-transfer complex. In case of the weak electron acceptor TNF, the reflection spectra exhibit only a broad unstructured absorbance up to 1400 nm, suggesting CT interactions without TMPD oxidation (*Figure 8*). Interestingly, the bulk polymers are not oxidized by air, oxygen or chlorine atmospheres, although the monomers are extremely oxygen-sensitive and are oxidized instantaneously on exposure to oxygen. Even solutions of the polymers in aprotic solvents are rather stable in air, whereas solutions in HCl turn dark blue rapidly, when not deoxygenated.

Conductivity studies

All untreated polymers are insulators with conductivities below the experimental range of sensitivity ($\sigma < 10^{-12}\,\Omega^{-1}\,cm^{-1}$). However, many electron-rich insulating polymers can be converted into conductive ones by oxidation ('doping')[19,20]. Iodine is one of the most efficient dopants known for conjugated polymers such as

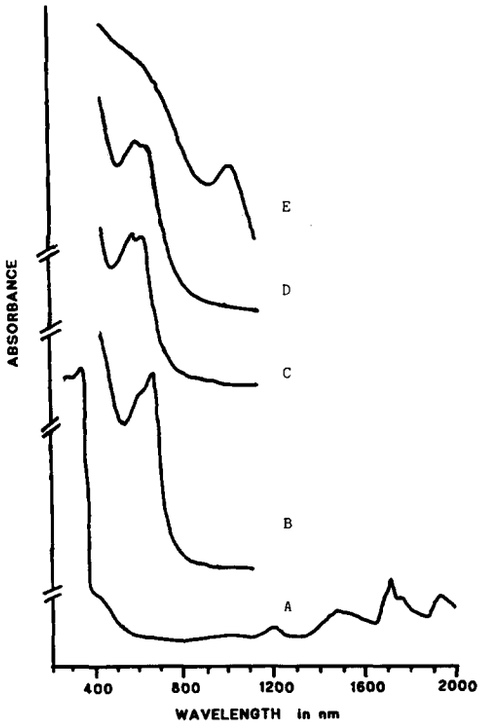

Figure 7 Reflection u.v./n.i.r. spectra of P-T2M (**17**): (a) background and pure polymer, (b) 1 mol of H_2O_2 added, (c) 1 mol of bromine added, (d) 1 mol of iodine added, (e) 10 mol of iodine added

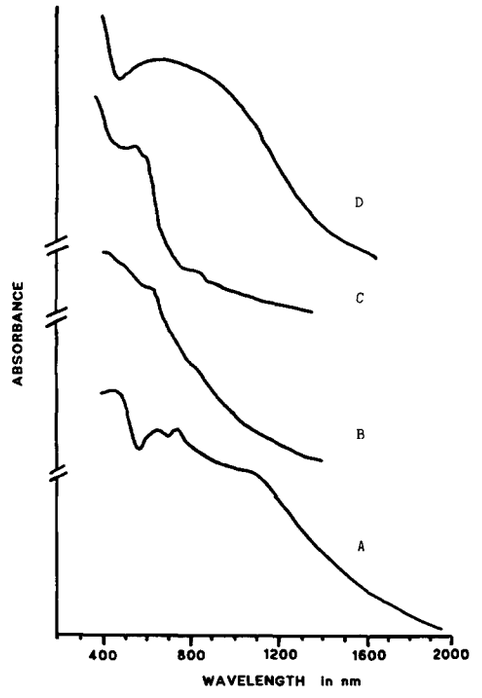

Figure 8 Reflection u.v./n.i.r. spectra of P-T2M (**17**): (a) 1 mol of TCNQ added, (b) 1 mol of TCNE added, (c) 1 mol of chloranil added, (d) 1 mol of 2,4,6-trinitrofluoroenone (TNF) added

polyacetylene, and additionally is known to form weakly conductive charge-transfer (CT) complexes with many polymers with electron donor groups. Thus, we have explored the conductivity of the polymer samples on exposure to iodine vapour. A representative plot of conductivity *versus* time of exposure to iodine is illustrated in *Figure 9*. The conductivity increases nearly six orders of magnitude, eventually reaching a final saturation value. The conductivity of the iodine-exposed polymers increased with temperature, indicating semiconducting properties.

The measured conductivities of 10^{-4}–$10^{-2}\,\Omega^{-1}\,cm^{-1}$ are considerably higher than those observed previously for CT complexes of iodine with many polymers[21–26], but much lower than iodine-doped conductive polymers such as polyacetylene or polyphenylene[19,20]. As all polymers containing 1,4-phenylenediamine units show comparable conductivities, independent of the molecular structure, the position of the phenylenediamine moiety in the polymers seems to be of no importance. The measured conductivities of polymers such as P-T2M (**17**), P-DMPD8 (**31**) and P-Et/DMPD (**35**) are the same within the accuracy of the experiments. This seems to apply as well on the density of functional groups. This phenomenon is best exemplified by comparison of P-T2M (**17**) and P-T6M (**19**) with their MMA-containing copolymers (**23**)–(**28**), all exhibiting maximal conductivities of 10^{-4}–$10^{-2}\,\Omega^{-1}\,cm^{-1}$. If decreased density of the functional group reduces the conductivity of the polymer–iodine complexes at all, the effect is only minor. These observations suggest that aggregation of radical cation units[27] in the polymers is not primarily responsible for the observed conductivity.

Long-term studies of iodine-doped polymers indicated the importance of iodine for maintaining conductivity. Once the maximum conductivity was obtained, the value stayed constant for weeks when stored in the presence of iodine. However, the conductivity of these compounds decreased upon standing in air. On exposing the decayed samples to iodine vapour again, the original conductivity was restored. Therefore, the observed conductivity depends upon reversibly bound iodine.

Large amounts of iodine are adsorbed by the 1,4-phenylenediamine-containing polymers, as indicated by a pronounced swelling of polymer samples after exposure to iodine vapour. *Table 8* depicts the uptake of iodine determined gravimetrically, after exposure of 30 mg of polymer to iodine vapour for 2 weeks. Up to 480% gain in weight is observed for the phenylenediamine polymers, whereas under the conditions applied, the amount of iodine adsorbed by PMMA or polystyrene is negligible. The values do not necessarily represent the maximum

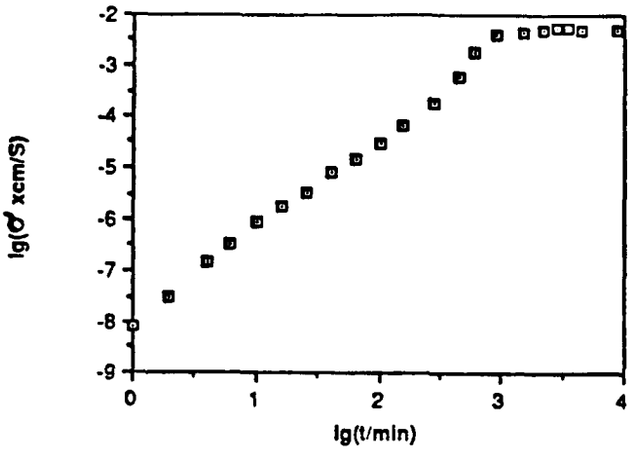

Figure 9 Conductivity of P-T2M as function of exposure time to iodine vapour

Table 8 Uptake of iodine of the studied polymers

Polymer		Iodine uptake	
		Per cent	I atoms per diamine
P-T2M (**17**)		480	10.0
P-T3M (**18**)		410	8.9
P-T6M (**19**)		380	9.6
P-T2S (**20**)		360	8.1
P-T3S (**21**)		290	6.8
P-T6S (**22**)		270	7.2
P-MMA-T2M-3	(**23**)	260	12.1
P-MMA-T2M-7	(**24**)	220	17.4
P-MMA-T2M-b15	(**27**)	210	31.3
P-MMA-T6M-4	(**25**)	250	14.1
P-MMA-T6M-7	(**26**)	180	15.2
P-MMA-T2M-b7	(**28**)	230	19.2
P-DMPD4		440	7.8
P-DMPD8		300	6.5
P-DMPD12		400	10.8
P-Et/DMPD		420	7.2
P-MVE/DMPD		340	6.7
PMMA		19	0.15
Polystyrene		22	0.2

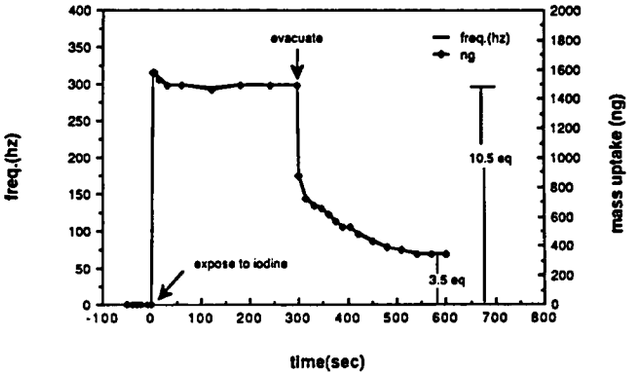

Figure 10 Frequency response of a piezoelectric quartz crystal coated with P-T2M, upon adsorption and desorption of iodine vapour. The film was prepared by addition of 10 μl of 0.1 mg/10 ml CH_2Cl_2 to the active surface of a 6 MHz AT crystal

iodine uptake, but provide a rough estimation of the amount of iodine that can be bound. The polymer backbone seems to be rather inert towards iodine, as the uptake is high for all types of polymers. The phenylenediamine moiety must be primarily responsible for iodine uptake. More significant amounts of iodine per phenylenediamine were even adsorbed in copolymers (**23**)–(**26**) of methyl methacrylate with T2M (**10**) or T6M (**13**), reaching 30 iodine atoms per phenylenediamine unit, suggesting the presence of polyiodide species.

The iodine uptake of 1,4-phenylene-diamine-containing polymers was investigated in more detail with P-T2M (**17**). The maximum conductivity of $5 \times 10^{-3}\,\Omega^{-1}\,cm^{-1}$ was reached after the uptake of iodine reaching 10 atoms of iodine per phenylenediamine group on long exposure. Such samples exhibit in their absorption spectra a new band at 1000 nm in addition to the 500–700 nm bands (*Figure 7*), pointing either to a polyiodide–poly(radical cation) CT complex, or to aggregation of the radical cation moieties[28]. By keeping the samples in vacuum for 4 days, six of the 10 iodines could be removed (determined gravimetrically), resulting in a loss of the 1000 nm band and a dramatic increase in conductivity. These results were corroborated by measurements performed on thin films of P-T2M deposited on a piezoelectric quartz crystal microbalance (QCM). The QCM comprises a thin plate of single crystal quartz (AT cut) sandwiched between two gold electrodes. Using conventional electronic circuits, the QCM can be induced to oscillate at a resonant frequency and mass changes at the gold electrodes can be determined from the shift in resonant frequency according to the Sauerbrey relationship[31]:

$$\Delta f = -\frac{2f_0^2\,\Delta m}{A(\rho_q \mu_q)^{1/2}}$$

where Δf is the measured frequency shift, f_0 the parent frequency of the quartz crystal, Δm the mass change, A the piezoelectrically active area, ρ_q the density of quartz (2.648 g cm^{-3}) and μ_q the shear modulus (2.947×10^{11} dyn cm^{-2} for AT-cut quartz). *Figure 10* shows that the maximal uptake of iodine is 10.5 atoms per polymer repeat unit, of which 7 are reversibly and 3.5 tightly bound. The stoichiometry of the tightly bound iodine suggests the presence of I_3^- counterions in this polymer. It might be speculated that not the neutral parent polymer but the oxidized polycationic species is the active host for iodine, in analogy to complexes of iodine and polyvinylpyridinium compounds or ionenes respectively[21]. Such behaviour would account for the quite uniform conductivities observed, and for the analogous results reported on carbazole-containing polymers[24].

CONCLUSIONS

Group-transfer polymerization proved to be the polymerization method of choice, to synthesize redox-active polymers and copolymers containing *N,N,N′,N′*-tetra-alky-1,4-phenylene-diamine, as otherwise side-reactions with the rather sensitive functional groups interfere. Although precursors and monomers are extremely air-sensitive, the polymers are (meta)stable in air. On oxidation, the polymers become stable poly(radical ions), which can be reversibly reduced. Hence, these polymers may be useful redox reagents. As the redox potentials studied by cyclic voltammetry are nearly independent of the molecular structure, regardless of whether monomers or polymers were studied, the polymer structure of such redox-active Wurster's blue polymers can be chosen freely, depending on additional properties wanted, such as solubility or mechanical strength. Owing to the low oxidation potentials, poly(radical ions) are obtained by oxidation with various 'mild' oxidants or electron acceptors, such as hydrogen peroxide, chloranil or TCNE. All polymers are able to find large amounts of iodine, most of it reversibly. The use of excess iodine as oxidant yielded polymers with conductivities of 10^{-4}–$10^{-2}\,\Omega^{-1}\,cm^{-1}$, up to 85% by weight iodine being absorbed. As the conductivities measured are virtually equal for all polymers studied, it is assumed that the main contribution to conductivity derives from polyiodide groups.

REFERENCES

1 Manecke, G. *Angew. Makromol. Chem.* 1968, **4/5**, 26
2 Manecke, G. and Storck, W. in 'Encyclopedia of Polymer Science and Engineering', (Eds. H. F. Mark, N. M. Bikales, C. G. Overberger, G. Menges and J. I. Kroschwitz), Wiley-Interscience, New York, 1986, Vol. 5, pp. 725–55

3 Willstätter, R. and Piccard, J. *Chem. Ber.* 1908, **37**, 4605
4 Michaelis, L. and Granick, S. *J. Am. Chem. Soc.* 1943, **65**, 1747
5 Kaufmann, F. B. *J. Am. Chem. Soc.* 1976, **98**, 5339
6 Klöpffer, W. and Rabenhorst, H. *J. Chem. Phys.* 1968, **49**, 156
7 Hörhold, H. H., Klee, J. and Bellstedt, *Z. Chem.* 1982, **22**, 166
8 Klee, J., Hörhold, H. H. and Schütz, H. *Acta Polym.* 1987, **38**, 293
9 Stewart, F. C. *J. Chem. Soc.* 1957, 1026; 'Beilstein', Vol. XIII, 4 suppl., 1085, p. 453
10 Nölting, E. *Chem. Ber.* 1885, **18**, 1143
11 Webster, O. W., Hertler, W. R., Sogah, D. Y., Farnham, W. B. and RajanBabu, T. V. *J. Am. Chem. Soc.* 1983, 5706
12 Dicker, I. B., Cohen, G. M., Farnham, W. B., Hertler, W. R., Langanis, E. D. and Sogah, D. Y. *Polym. Prepr. Am. Chem. Soc.* 1987, **28**(1), 106
13 Müller, M. A. and Stickler, M. *Makromol. Chem. Rapid Commun.* 1986, **7**, 575
14 Hertler, W. R., RajanBabu, T. V., Ovenall, D. W., Ready, G. S. and Sogah, D. Y. *J. Am. Chem. Soc.* 1988, **110**, 5841
15 Ueda, N., Natsume, B., Yanagiuchi, K., Sakata, Y., Enoki, T., Saito, G., Inokuchi, H. and Misumi, S. *Bull. Chem. Soc. Jpn* 1983, **56**, 775
16 Breslow, R. *Pure Appl. Chem.* 1982, **54**, 927
17 Bent, R. L. *et al. J. Am. Chem. Soc.* 1951, **73**, 3100
18 Daum, P. and Murray, R. W. *J. Electroanal. Chem.* 1979, **103**, 289; *J. Phys. Chem.* 1981, **85**, 389
19 Duke, C. B. and Gibson, H. W. in 'Kirk-Othmer, Encyclopedia of Chemical Technology', 3rd Edn., Wiley, New York, 1982, Vol. 18, pp. 755–93
20 Frommer, J. E. and Chance, R. R. in 'Encyclopedia of Polymer Science and Engineering', (Eds. H. F. Mark, N. M. Bikales, C. G. Overberger, G. Menges and J. I. Kroschwitz), Wiley-Interscience, New York, 1986, Vol. 5, pp. 462–507
21 Mainthia, S. B., Kronick, P. L. and Labes, M. M. *J. Chem. Phys.* 1964, **41**, 2206
22 Herrmann, A. M. and Rembaum, A. *J. Polym. Sci.* (*C*) 1967, **17**, 107
23 Knoesel, R., Gebus, B., Roth, J. P. and Parrod, J. *Bull. Soc. Chim. Fr.* 1969, 294
24 Subramaniam, P., Sasakawa, T., Ikeda, T., Tazuke, S. and Srinivasan, M. *J. Polym. Sci.* (*A*) 1987, **25**, 1463
25 Glatzhofer, D. T. and Longone, D. T. *J. Polym. Sci.* (*A*) 1986, **24**, 947
26 Thakur, M. *Macromolecules* 1988, **21**, 661
27 Greene, R. L. and Street, G. B. *Science* 1984, **226**, 651
28 Iida, Y. and Matsunaga, Y. *Bull. Chem. Soc. Jpn* 1968, **41**, 2615
29 Tanaka, J. and Mizuno, M. *Bull. Chem. Soc. Jpn* 1969, **42**, 1841
30 Ward, M. D. *J. Phys. Chem.* 1988, **92**, 2049
31 Sauerbrey, G. *Z. Phys.* 1959, **155**, 206